2010 IEEE International Conference on Robotics and Automation
Anchorage Convention District
May 3-8, 2010, Anchorage, Alaska, USA

Towards 100G with PKM. Is actuation redundancy a good solution for pick-and-place?

David Corbel, Marc Gouttefarde, Olivier Company and François Pierrot
LIRMM, Univ. Montpellier 2, CNRS
161 rue Ada, 34392 Montpellier, France
Email: david.corbel@lirmm.fr
Phone: +33/0 467 41 85 85
Fax: +33/0 467 41 85 00

Abstract— **This paper analyzes the possible contribution of actuation redundancy in obtaining very high acceleration with Parallel Kinematic Machines (PKM). This study is based on redundant and non-redundant Delta/Par4-like robots (frequently used for pick-and-place applications). The dynamic model, valid for both redundant and non-redundant robots, is used to analyze the traveling plate acceleration capabilities: (i) at zero speed and in any directions, (ii) at zero speed in the "best" direction. The results show that actuation redundancy allows to homogenize the dynamic capabilities throughout the workspace and to increase the traveling plate acceleration capability. Finally, the design of a redundant Delta/Par4-like robot optimized for typical pick-and-place trajectories is presented.**

I. INTRODUCTION

Parallel robots (or PKM, for "Parallel Kinematic Machines") are widely recognized as efficient machines for applications that require high speed and high accelerations. This is especially true for PKM similar to Delta [1] or Par4 [2]: both robots feature lightweight mechanical components combined with good structural stiffness and can reach above 10 m/s velocity and 150 m/s^2 acceleration in pick-and-place applications. Indeed, they both rely on **R**-(SS)^2 (where **R** represents a revolute joint and S a spherical joint) chains which provide the following advantages:

- Motors are rigidly fixed on the base and their mass does not impair fast motions;
- The actuated **R** joints move arms whose length is a kind of "natural velocity amplifier" (the longest the arm is, the highest its tip velocity is);
- The rods, linked by S joints to the arms and to the traveling plate, essentially transmit pure forces and no torque; working in tension and compression only, they can be made very thin and light.

It has been shown that for reaching high accelerations such PKM have to be analyzed in the light of their dynamic models and not by considering their kinematics only [1] [3]. In fact, even the inertia of their actuation systems have to be precisely accounted for since it represents a large part of the overall inertia. However, even though a PKM has been properly designed by resorting to a dynamic-model-based optimization process (*e.g.*, finding the robot geometry which gives the lowest peak torque over the workspace for a given motion) it remains true that PKM dynamic capabilities vary a lot throughout the workspace. Redundancy might be a way to overcome this problem and even to reach higher acceleration in general. With PKM, the concept of "redundancy" is quite complex as it covers a large variety of situations [4]:

- Kinematic redundancy, which is similar to the case of serial robots, that is, for a given end-effector velocity and a given pose, there are an infinite number of corresponding joint velocities;
- Measurement redundancy, which corresponds to machines featuring more position sensors than end-effector degrees of freedom (*e.g.*, some passive joints may be equipped with sensors);
- Actuation redundancy, where, for a given force/wrench acting on the end-effector and a given pose, there are an infinite number of corresponding joint forces/torques.

his paper considers *actuation redundancy*. Actuation redundancy has been used in the past to improve PKM in regards of kinetostatic performances [5] [6] [7], operational stiffness [8] [9], singularity avoidance [10] [9], backlash control [11] or acceleration capability [12]. Here, the following question is analyzed, in the case of Delta/Par4-like mechanisms: is it possible to obtain with redundant PKM a better acceleration capability than with non-redundant PKM? Indeed, answering this question is not obvious since *actuation redundancy* means more *available torque* but *more inertia* too.

Kinematic and dynamic models will be firstly recalled in section II and this will lead to a dynamic model which encompasses both the redundant and non-redundant cases. This model is then used in four different ways: (i) Analyzing the acceleration capability available at zero speed and in any direction, (ii) Analyzing the highest acceleration capability at zero speed (in the "best" direction), (iii) Analyzing the ratio between these two capabilities at zero speed (homogeneity of the acceleration capabilities) and (iv) Analyzing the torque required along a typical pick-and-place path. The first three analyses compare 3-dof robots with 3, 4 and 6 actuators (section IV) and resort to zonotopes rather than to ellipsoids as will be explained in section III. The fourth analysis (iv) considers a 3-dof robot with 4 motors (section V) and shows that it might be possible to reach up to 100G in a pick-and-place application with a redundant PKM.

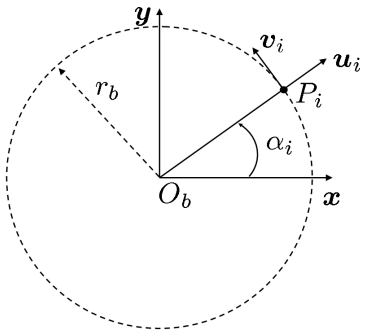

(a) Overhead view

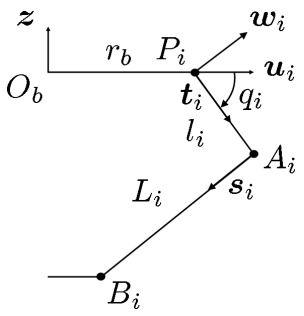

(b) Side view

Fig. 1. Delta/Par4-like robot geometric parameters

II. Delta/Par4-like robots

In this section, the modeling of Delta/Par4-like robots, redundant or not, is presented. Only the Inverse Kinematic Model (IKM), the inverse Jacobian matrix and the Direct Dynamic Model (DDM) are presented since, in the case of redundant robots, a unique solution exists neither for the Direct Kinematics nor for the Inverse Dynamics. Some information regarding the Direct Kinematic Model (DKM) of redundantly actuated parallel robots can be found in [13].

In the following, n denotes the number of actuators.

A. Parametrization

The geometric parameters involved in the modeling of Delta/Par4-like robots are shown in Fig. 1 ($i = 1, .., n$). In the modeling, the forearms, which are spatial parallelograms, are replaced by simple rods.

The joint center locations are represented by the points P_i, A_i and B_i whose coordinates in the fixed Cartesian frame O_b - $\boldsymbol{xyz}$ are:

$$\boldsymbol{p}_i = r_b \begin{bmatrix} \cos\alpha_i & \sin\alpha_i & 0 \end{bmatrix}^T, \tag{1}$$

$$\boldsymbol{a}_i = \boldsymbol{p}_i + l_i \begin{bmatrix} \cos\alpha_i \cos q_i & \sin\alpha_i \cos q_i & \sin q_i \end{bmatrix}^T, \tag{2}$$

$$\boldsymbol{b}_i = \begin{bmatrix} r_{tp}\cos\alpha_i + x & r_{tp}\sin\alpha_i + y & z \end{bmatrix}^T, \tag{3}$$

where r_b, r_{tp}, α_i, l_i, L_i, q_i and $\begin{bmatrix} x & y & z \end{bmatrix}^T$ denote the base radius, the traveling plate radius, the orientation of the actuator axes ($\alpha_i = \frac{2(i-1)\pi}{n}$), the arm length, the forearm length, the actuated joint variable and the traveling plate position vector, respectively.

A frame P_i - $\boldsymbol{u_i v_i z}$ is attached to each actuator such that the vectors $\boldsymbol{u}_i$ and $\boldsymbol{v}_i$ are given by:

$$\boldsymbol{u}_i = \begin{bmatrix} \cos\alpha_i & \sin\alpha_i & 0 \end{bmatrix}^T, \tag{4}$$

$$\boldsymbol{v}_i = \begin{bmatrix} -\sin\alpha_i & \cos\alpha_i & 0 \end{bmatrix}^T, \tag{5}$$

where $\boldsymbol{v}_i$ is directed along the actuator axis.

The unit vectors $\boldsymbol{t}_i$, $\boldsymbol{s}_i$ and $\boldsymbol{w}_i$ are defined by:

$$\boldsymbol{t}_i = \frac{\overline{P_i A_i}}{l_i}, \tag{6}$$

$$\boldsymbol{s}_i = \frac{\overline{A_i B_i}}{L_i}, \tag{7}$$

and

$$\boldsymbol{w}_i = \boldsymbol{t}_i \times \boldsymbol{v}_i. \tag{8}$$

B. Inverse Kinematics

In order to avoid the mathematical singularities of the Delta/Par4-like robots classical IKM [14], the IKM proposed by Codourey [15] is used. Being given the position of the traveling plate, this IKM computes the actuated joint variables q_i as follows:

$$q_i = \begin{cases} asin\left(\frac{h}{l_i}\right) & , \quad d - r_b \geq 0, \\ \pi - asin\left(\frac{h}{l_i}\right) & , \quad d - r_b < 0, \end{cases} \tag{9}$$

with

$$h = \frac{A - Bd}{2z_{B_i}}, \tag{10}$$

$$d = \frac{b + \sqrt{b^2 - ac}}{a}, \tag{11}$$

and

$$a = 4z_{B_i}^2 + B^2, \tag{12}$$

$$b = 4r_b z_{B_i} + AB, \tag{13}$$

$$c = A^2 + 4r_b^2 z_{B_i}^2 - 4z_{B_i}^2 l_i^2, \tag{14}$$

$$A = l_i^2 - L_i^2 - r_b^2 + x_{B_i}^2 + y_{B_i}^2 + z_{B_i}^2, \tag{15}$$

$$B = 2x_{B_i} - 2r_b, \tag{16}$$

where x_{B_i}, y_{B_i} and z_{B_i} are the coordinates of points B_i in the frame P_i - $\boldsymbol{u_i v_i z}$.

C. Inverse Jacobian Matrix

The inverse jacobian matrix $\boldsymbol{J}_m$ maps the traveling plate velocity vector $\dot{\boldsymbol{x}}$ to the joint velocity vector $\dot{\boldsymbol{q}}$:

$$\dot{\boldsymbol{q}} = \boldsymbol{J}_m \dot{\boldsymbol{x}}, \tag{17}$$

with

$$\boldsymbol{J}_m = \boldsymbol{J}_q^{-1} \boldsymbol{J}_x. \tag{18}$$

The matrices $\boldsymbol{J}_q$ and $\boldsymbol{J}_x$ can be determined by using the equiprojectivity property of the velocities on the forearms:

$$\boldsymbol{v}_{A_i} \cdot \boldsymbol{s}_i = \boldsymbol{v}_{B_i} \cdot \boldsymbol{s}_i, \tag{19}$$

where $\cdot$ denotes the dot product, $\boldsymbol{v}_{A_i}$ and $\boldsymbol{v}_{B_i}$ are the velocities vectors of points A_i and B_i.

$\boldsymbol{J}_q$ and $\boldsymbol{J}_x$ can be written as follows:

$$\boldsymbol{J}_q = \begin{bmatrix} l_1 \boldsymbol{w}_1^T \boldsymbol{s}_1 & & \boldsymbol{0} \\ & \ddots & \\ \boldsymbol{0} & & l_n \boldsymbol{w}_n^T \boldsymbol{s}_n \end{bmatrix}, \tag{20}$$

$$\boldsymbol{J}_x = \begin{bmatrix} \boldsymbol{s}_1 & \dots & \boldsymbol{s}_n \end{bmatrix}^T, \tag{21}$$

Finally, the inverse jacobian matrix $\boldsymbol{J}_m$ is obtained as:

$$\boldsymbol{J}_m = \begin{bmatrix} \frac{\boldsymbol{s}_1}{l_1 \boldsymbol{w}_1^T \boldsymbol{s}_1} & \cdots & \frac{\boldsymbol{s}_n}{l_n \boldsymbol{w}_n^T \boldsymbol{s}_n} \end{bmatrix}^T. \tag{22}$$

When $\boldsymbol{J}_m$ is a square matrix, it is the inverse of the jacobian matrix $\boldsymbol{J}$ which maps the joint velocity vector $\dot{\boldsymbol{q}}$ to the velocity vector of the traveling plate $\dot{\boldsymbol{x}}$. In the case of redundant robots, $\boldsymbol{J}_m$ is not square and cannot be inverted.

D. Simplified Direct Dynamics

Several hypotheses can be made in order to simplify the calculation of the DDM. First, joint friction is neglected. The inertia of the forearms I_f is also neglected and their mass m_f is split in two parts each being artificially considered to be located at both ends of the forearms as shown in Fig. 2. Hence, half of the mass is transferred to the end of the arm whereas the other half is transferred to the traveling plate. These assumptions are discussed in [3] and in [16] and have proven to be consistent with the technologies in use for such robots (that is: the difference between models with or without those assumptions is in the range of a few percents). Finally, gravity is not taken into account because the case studies will consider very high acceleration (up to 100G), and that allows to neglect gravity.

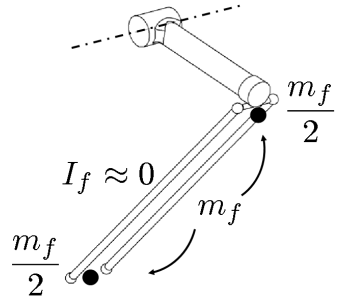

Fig. 2. Forearm mass consider as point mass

1) Arm equilibrium: the relationship between the actuator torque vector $\boldsymbol{\Gamma}$ and acceleration vector $\ddot{\boldsymbol{q}}$ is

$$\boldsymbol{\Gamma} - {\boldsymbol{J}_q}^T \boldsymbol{f} = \boldsymbol{I}_{tot} \ddot{\boldsymbol{q}}, \tag{23}$$

where $\boldsymbol{f}$ is the vector of the forces, due to the acceleration of the traveling plate, applied on the arm at points A_i. The matrix $\boldsymbol{I}_{tot}$ is a diagonal matrix. The terms on its main diagonal are:

$$I_{tot} = I_{act} + I_{arm} + \frac{l_i^2 m_f}{2}, \tag{24}$$

where I_{act} and I_{arm} are the inertia of the actuators and the inertia of the arms, respectively.

2) Traveling plate equilibrium: the equation of motion of the traveling plate is:

$$\boldsymbol{J}_x^T \boldsymbol{f} = \boldsymbol{M}_{tot} \ddot{\boldsymbol{x}}, \tag{25}$$

where $\boldsymbol{M}_{tot}$ is a diagonal matrix with diagonal terms, m_{tot}, consisting of the mass of the traveling plate m_{tp} and n times half the mass of the forearm:

$$m_{tot} = m_{tp} + n \frac{m_f}{2}. \tag{26}$$

3) Complete equilibrium: From (23), $\boldsymbol{f}$ can be expressed as a function of the actuator torques $\boldsymbol{\Gamma}$ and the angular accelerations $\ddot{\boldsymbol{q}}$

$$\boldsymbol{f} = \boldsymbol{J}_q^{-T} \left(\boldsymbol{\Gamma} - \boldsymbol{I}_{tot} \ddot{\boldsymbol{q}} \right), \tag{27}$$

provided that $\boldsymbol{J}_q$ is not singular.

Combining (25) and (27) gives the following relation:

$$\begin{aligned} \boldsymbol{M}_{tot} \ddot{\boldsymbol{x}} &= \boldsymbol{J}_x^T \boldsymbol{J}_q^{-T} \left(\boldsymbol{\Gamma} - \boldsymbol{I}_{tot} \ddot{\boldsymbol{q}} \right) \\ &= \boldsymbol{J}_m^T \left(\boldsymbol{\Gamma} - \boldsymbol{I}_{tot} \ddot{\boldsymbol{q}} \right). \end{aligned} \tag{28}$$

Differentiating (17) with respect to time, the relation between the angular accelerations $\ddot{\boldsymbol{q}}$ and the traveling plate velocity $\dot{\boldsymbol{x}}$ and acceleration $\ddot{\boldsymbol{x}}$ vectors is found as follows:

$$\ddot{\boldsymbol{q}} = \boldsymbol{J}_m \ddot{\boldsymbol{x}} + \dot{\boldsymbol{J}}_m \dot{\boldsymbol{x}}, \tag{29}$$

with

$$\dot{\boldsymbol{J}}_m = \begin{bmatrix} \frac{1}{l_1} \left(\frac{\dot{\boldsymbol{r}}_1^T \boldsymbol{s}_1 + \boldsymbol{r}_1^T \dot{\boldsymbol{s}}_1}{(\boldsymbol{r}_1^T \boldsymbol{s}_1)^2} \right) \boldsymbol{s}_1^T + \frac{1}{l_1 \boldsymbol{r}_1^T \boldsymbol{s}_1} \dot{\boldsymbol{s}}_1^T \\ \vdots \\ \frac{1}{l_n} \left(\frac{\dot{\boldsymbol{r}}_n^T \boldsymbol{s}_n + \boldsymbol{r}_n^T \dot{\boldsymbol{s}}_n}{(\boldsymbol{r}_n^T \boldsymbol{s}_n)^2} \right) \boldsymbol{s}_n^T + \frac{1}{l_n \boldsymbol{r}_n^T \boldsymbol{s}_n} \dot{\boldsymbol{s}}_n^T \end{bmatrix}. \tag{30}$$

Finally, the expression of the DDM is:

$$\ddot{\boldsymbol{x}} = \left(\boldsymbol{M}_{tot} + \boldsymbol{J}_m^T \boldsymbol{I}_{tot} \boldsymbol{J}_m \right)^{-1} \boldsymbol{J}_m^T \left(\boldsymbol{\Gamma} - \boldsymbol{I}_{tot} \dot{\boldsymbol{J}}_m \dot{\boldsymbol{x}} \right). \tag{31}$$

III. Comparison indexes

In the next section, the dynamic capabilities of three Delta/Par4-like robots will be compared. The present section defines the indexes used to carry out this comparison. The method used to compute these indexes is also briefly presented. Note that these indexes have the same meaning both for redundant and non-redundant robots.

A. Definitions of the Indexes

Equation (31) can be rewritten as follows:

$$\ddot{\boldsymbol{x}} = \boldsymbol{H} \boldsymbol{\Gamma} - \boldsymbol{A} \dot{\boldsymbol{x}}, \tag{32}$$

where $\boldsymbol{H}$ is a $3 \times n$ matrix. Investigating the dynamic capability of a Delta/Par4-like robot by means of (32) would be a complex task on its own. Therefore, in order to define comparison indexes, let us consider (32) with a null traveling plate velocity vector:

$$\ddot{\boldsymbol{x}} = \boldsymbol{H} \boldsymbol{\Gamma}. \tag{33}$$

This amounts to studying the acceleration capability of the robot at a standstill, e.g. at the starting point of a high-speed

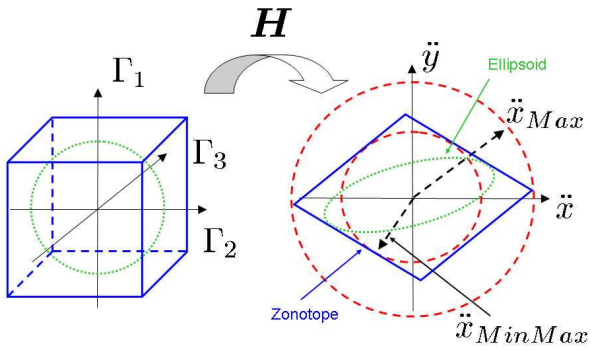

Fig. 3. Illustration of the comparison indexes

pick-and-place trajectory—at which a very high acceleration is specifically required, however.

Equation (33) provides a linear relation which enables the determination of the set of possible traveling plate accelerations. In fact, each actuator has a maximum torque Γ_{max} so that the *set of available actuator torques* is:

$$[\boldsymbol{\Gamma}] = \{\boldsymbol{\Gamma} \mid \Gamma_i \in [-\Gamma_{i_{max}}, \Gamma_{i_{max}}], \ 1 \leq i \leq n\}. \quad (34)$$

This bounded set of available torques limits the possible traveling plate accelerations and, according to (33), the corresponding *set of available traveling plate accelerations* is:

$$\mathcal{Z} = \boldsymbol{H}[\boldsymbol{\Gamma}] = \{\ddot{\boldsymbol{x}} \mid \exists\, \boldsymbol{\Gamma} \in [\boldsymbol{\Gamma}] \text{ such that } \ddot{\boldsymbol{x}} = \boldsymbol{H}\boldsymbol{\Gamma}\}. \quad (35)$$

The first index, used in section IV-C for comparison purposes, is the *min-max traveling plate acceleration*:

$$\boxed{\ddot{x}_{MinMax} = \min_{\boldsymbol{u}\in\mathbb{R}^3, \|\boldsymbol{u}\|=1} \left(\max_{\alpha \geq 0} \{\alpha \mid \alpha \boldsymbol{u} \in \mathcal{Z}\} \right)}. \quad (36)$$

It is the radius of the largest ball centered at the origin and fully included in the set of available traveling plate accelerations $\mathcal{Z}$ (Fig. 3). Therefore, being given that $|\Gamma_i| \leq \Gamma_{i_{max}}$ for each actuator, an acceleration vector of magnitude $\ddot{x}_{MinMax}$ can be generated at the traveling plate in *any* direction of the task space.

The second index, called the *maximum possible traveling plate acceleration*, is defined as:

$$\boxed{\ddot{x}_{Max} = \max_{\ddot{\boldsymbol{x}}\in\mathcal{Z}}(\|\ddot{\boldsymbol{x}}\|)}, \quad (37)$$

where $\|\cdot\|$ denotes the 2-norm. It will be used in section IV-D to compare three Delta/Par4-like robots. Note that $\ddot{x}_{Max}$ is equal to the radius of the smallest ball, centered at the origin, that fully contains $\mathcal{Z}$ (Fig. 3). It is important to remark here that zonotopes are used instead of ellipsoids [17] in order to encompass the real maximal robot capabilities.

B. Computation of the Indexes

Being the image of the box $[\boldsymbol{\Gamma}]$ under the linear transformation $\boldsymbol{H}$ (where $\boldsymbol{H}$ is not square for $n > 3$ actuators), the set of available traveling plate accelerations $\mathcal{Z}$ is a convex polytope. This type of polytope is equivalent to the ones studied, e.g. in [18], when analyzing the wrench capability of redundant parallel robots. Besides, in a study of the wrench capability of parallel cable-driven robots, Bouchard [19] recently pointed out the nature of the polytopes such as $\mathcal{Z}$: they are zonotopes. Based on this useful observation, the latter reference proposed a method to determine the facet-defining hyperplanes of a zonotope yielding a representation of $\mathcal{Z}$ as the (bounded) solution set of a finite system of linear inequalities:

$$\mathcal{Z} = \{\ddot{\boldsymbol{x}} \mid \boldsymbol{C}\ddot{\boldsymbol{x}} \leq \boldsymbol{d}\}, \quad (38)$$

where $\boldsymbol{C}$ is a $p \times 3$ matrix and $\boldsymbol{d}$ a p-dimensional vector, p being the number of inequalities in the system. Provided that the origin $\ddot{\boldsymbol{x}} = \boldsymbol{0}$ belongs to $\mathcal{Z}$, all the components of $\boldsymbol{d}$ are nonnegative and (38) allows us to determine the min-max traveling plate acceleration as:

$$\ddot{x}_{MinMax} = \min_{1\leq j\leq q} \frac{d_j}{\|\boldsymbol{c}_j^T\|}, \quad (39)$$

where $\boldsymbol{c}_j^T$ denotes the jth line of $\boldsymbol{C}$ and d_j the jth component of $\boldsymbol{d}$.

Finally, the maximum possible traveling plate acceleration $\ddot{x}_{Max}$ can be found by first computing the images of the vertices of $[\boldsymbol{\Gamma}]$ under the linear transformation $\boldsymbol{H}$ and then by finding the one having the greater norm, $\ddot{x}_{Max}$ being equal to this norm.

IV. Dynamic Comparison

Three robots are compared in this section: a non-redundant Delta robot (NR, Fig. 4a), a redundant robot with 4 actuators, which could be seen as a Delta with one additional chain or a Par4 with a rigid traveling plate (R4, Fig. 4b) and a redundant robot with 6 actuators (R6, Fig. 4c). This section addresses the following questions: (i) can actuation redundancy improve the dynamic capabilities of a Delta/Par4-like robot? and (ii) if yes, which one among R4 and R6 is the solution yielding the best capabilities?

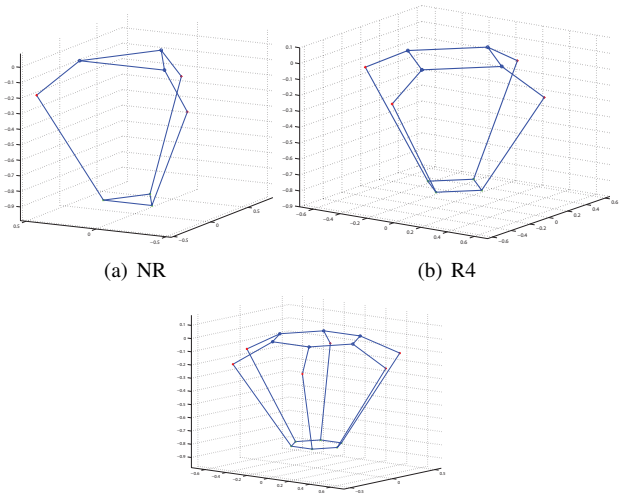

(a) NR (b) R4

(c) R6

Fig. 4. Matlab Sketch of the Delta/Par4-like robots

TABLE I

GEOMETRIC PARAMETERS

r_b (m)	r_{tp} (m)	l_i (m)	L_i (m)
0.350	0.100	0.350	0.800

TABLE II

DYNAMIC PARAMETERS

	NR	R4	R6
M_{tp} (kg)	0.6	0.6	0.6
I_{act} (kg·m ^{2})	0.004	0.003	0.002
I_{arm} (kg·m ^{2})	0.094	0.071	0.047
$M_{forearm}$ (kg)	0.4	0.3	0.2
Γ_{max} (N·m)	120	90	60

A. Geometric and dynamic parameters

Table I presents the geometric parameters of the three considered robots. These parameters are chosen as similar to those of the Par4 prototype built at the LIRMM [2]. If the geometric parameters of the three robots are the same, the dynamic parameters need to be adapted. Indeed, comparing fairly non-redundant and redundant robots requires that a relationship is established between the values of their dynamic parameters (Zhao and Gao do not make the same choice for the comparison of a 8**P**SS redundant parallel manipulator and its non-redundant counterpart [20]). The invariant selected here is the "total available torque", that is the sum of the maximum torque of the n motors. This means that if the sum of the maximum torques provided by the actuators for the non-redundant robot is equal to 1, the sum of the maximum torques for the redundant robots has to be equal to 1 too. In other words, more motors means smaller motors so that the total torque remains constant. Moreover, the ratio torque/inertia of the actuators is considered to be constant. As the actuator torques decrease from NR to R6, the inertia of the arms and the mass of the forearms can decrease too as shown in Table II.

B. Simulations

The simulations consist in:

(i) create a grid of points (x, y, z) included in the defined workspace (a cylinder of 300 mm radius and 100 mm height),

(ii) calculate for each point the value of both indexes ($\ddot{x}_{MinMax}$, $\ddot{x}_{Max}$) for the three robots,

(iii) calculate the ratios between NR, R4 and R6 indexes.

C. Min-Max Traveling Plate Acceleration

The first comparison index is the min-max traveling plate acceleration defined in section III-A.

The ratios are calculated as follows:

$$\eta^a_{\text{NR/R4}}(\boldsymbol{x}) = \frac{\ddot{x}_{MinMax_{\text{R4}}}(\boldsymbol{x}) - \ddot{x}_{MinMax_{\text{NR}}}(\boldsymbol{x})}{\ddot{x}_{MinMax_{\text{NR}}}(\boldsymbol{x})}, \quad (40)$$

TABLE III

COMPARING MIN-MAX TRAVELING PLATE ACCELERATION

$\eta^a_{\text{NR/R4}}$		$\eta^a_{\text{NR/R6}}$		$\eta^a_{\text{R4/R6}}$	
min	max	min	max	min	max
+12%	+23%	+22%	+30%	+4%	+9%

TABLE IV

COMPARING MAX TRAVELING PLATE ACCELERATION

$\eta^b_{\text{NR/R4}}$		$\eta^b_{\text{NR/R6}}$		$\eta^b_{\text{R4/R6}}$	
min	max	min	max	min	max
-2.3%	2.1%	-3.6%	-7.1%	-4.4%	-5.7%

$$\eta^a_{\text{NR/R6}}(\boldsymbol{x}) = \frac{\ddot{x}_{MinMax_{\text{R6}}}(\boldsymbol{x}) - \ddot{x}_{MinMax_{\text{NR}}}(\boldsymbol{x})}{\ddot{x}_{MinMax_{\text{NR}}}(\boldsymbol{x})}, \quad (41)$$

$$\eta^a_{\text{R4/R6}}(\boldsymbol{x}) = \frac{\ddot{x}_{MinMax_{\text{R6}}}(\boldsymbol{x}) - \ddot{x}_{MinMax_{\text{R4}}}(\boldsymbol{x})}{\ddot{x}_{MinMax_{\text{R4}}}(\boldsymbol{x})}. \quad (42)$$

Table III presents the minimum and the maximum values of the ratios over the considered workspace. These results show an important improvement of the acceleration capability of R4 and R6 compared to NR. Indeed, with only one redundant motor, R4 shows up to 23% improvement compared to NR. Moreover, R6 has the best min-max acceleration capability; however it needs 2 actuators more than R4 to improve the performance by 4 to 10% only.

D. Maximum Possible Traveling Plate Acceleration

Now, let us consider the maximum possible traveling plate acceleration defined in section III-A.

The ratios are calculated at each point $\boldsymbol{x}$ as follows:

$$\eta^b_{\text{NR/R4}}(\boldsymbol{x}) = \frac{\ddot{x}_{Max_{\text{R4}}}(\boldsymbol{x}) - \ddot{x}_{Max_{\text{NR}}}(\boldsymbol{x})}{\ddot{x}_{Max_{\text{NR}}}(\boldsymbol{x})}, \quad (43)$$

$$\eta^b_{\text{NR/R6}}(\boldsymbol{x}) = \frac{\ddot{x}_{Max_{\text{R6}}}(\boldsymbol{x}) - \ddot{x}_{Max_{\text{NR}}}(\boldsymbol{x})}{\ddot{x}_{Max_{\text{NR}}}(\boldsymbol{x})}, \quad (44)$$

$$\eta^b_{\text{R4/R6}}(\boldsymbol{x}) = \frac{\ddot{x}_{Max_{\text{R6}}}(\boldsymbol{x}) - \ddot{x}_{Max_{\text{R4}}}(\boldsymbol{x})}{\ddot{x}_{Max_{\text{R4}}}(\boldsymbol{x})}. \quad (45)$$

Table IV presents the minimum and the maximum values of the ratios obtained over the considered workspace. These results show that, contrary to the previous results, R6 is the worse in term of maximum possible acceleration even though the differences between the three robots are small. R6 is about 5% less efficient than NR; R4 is quite similar to NR.

E. Min-max Acceleration and Maximum Possible Acceleration

The last comparison between the three robots consists in comparing the ratios between the maximum possible acceleration $\ddot{x}_{Max}(\boldsymbol{x})$ and the min-max acceleration $\ddot{x}_{MinMax}(\boldsymbol{x})$ throughout the workspace:

$$\eta^c_{\text{NR}}(\boldsymbol{x}) = \frac{\ddot{x}_{Max_{\text{NR}}}(\boldsymbol{x})}{\ddot{x}_{MinMax_{\text{NR}}}(\boldsymbol{x})}, \quad (46)$$

TABLE V

COMPARING THE RATIO BETWEEN MAXIMUM POSSIBLE ACCELERATION AND MIN-MAX ACCELERATION

$\eta^c_{\text{NR}}(\boldsymbol{x})$		$\eta^c_{\text{R4}}(\boldsymbol{x})$		$\eta^c_{\text{R6}}(\boldsymbol{x})$	
min	max	min	max	min	max
1.80	2.17	1.53	1.88	1.33	1.64

$$\eta^c_{\text{R4}}(\boldsymbol{x}) = \frac{\ddot{x}_{Max_{\text{R4}}}(\boldsymbol{x})}{\ddot{x}_{MinMax_{\text{R4}}}(\boldsymbol{x})}, \tag{47}$$

$$\eta^c_{\text{R6}}(\boldsymbol{x}) = \frac{\ddot{x}_{Max_{\text{R6}}}(\boldsymbol{x})}{\ddot{x}_{MinMax_{\text{R6}}}(\boldsymbol{x})}. \tag{48}$$

Table V presents the minimum and the maximum values of these ratios. These results show that actuation redundancy allows to homogenize the dynamic capabilities of robots. A ratio equal to 1 means the min-max acceleration is equal to the max acceleration which is, *a priori*, the best case for a versatile robot. The table shows that the ratios of R4 and R6 are closer to 1 than the ratio of NR. R6 is still the best one.

F. Conclusion

These results show that actuation redundancy seems to homogenize the acceleration capabilities by increasing the min-max traveling plate acceleration across the workspace which comes closer to the maximum possible acceleration. Moreover, adding only one redundant chain is sufficient to have better dynamic capabilities. The cost of adding 2 or more chains is too high compared to the benefits in terms of acceleration capabilities. Therefore, R4 is selected. This choice allows us to obtain better dynamic performances than that of NR at a modest extra cost.

V. TOWARDS 100G PICK-AND-PLACE

The goal of this section is to select, among a finite set of values of R4 geometric parameters, the ones allowing the traveling plate to reach a 100G acceleration with the smallest torques. To this end, some trajectories with a maximum acceleration of 100G are defined. Then the actuator torques needed along the trajectories are calculated for several values of the geometric parameters. Finally, the parameters for which the peak torque is minimal are chosen.

Finding the torque corresponding to a given situation on the trajectory (that is: $\boldsymbol{x}$, $\dot{\boldsymbol{x}}$, $\ddot{\boldsymbol{x}}$, with $\dot{\boldsymbol{x}} \neq 0$) requires to invert equation (32); there exist several techniques to do so and a pseudo-inversion is chosen here. This gives a solution for $\boldsymbol{\Gamma}$ with a minimal 2-norm.

$$\boldsymbol{\Gamma} = \boldsymbol{H}^{+}(\ddot{\boldsymbol{x}} + \boldsymbol{A}\dot{\boldsymbol{x}}). \tag{49}$$

A solution with a minimal infinite-norm could be searched for as well. By definition, this would lead to a smaller value for the maximum torque but could create large changes in the components of $\boldsymbol{\Gamma}$ from one point to the next one along the trajectory, making this option less satisfactory in the view of robot control. A reader interested in control techniques suitable for redundantly actuated PKM should refer to [21] where sophisticated and efficient approaches are proposed.

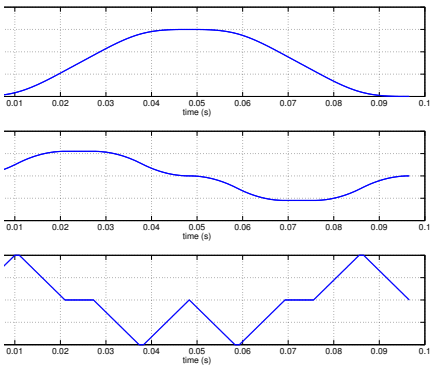

Fig. 5. Trajectory with 100G acceleration

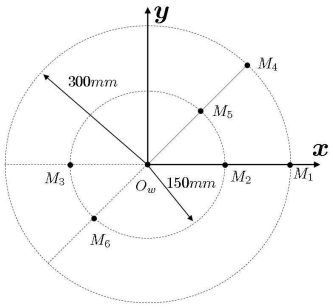

Fig. 6. Extreme points of the trajectories

A. Case study

The robot workspace must include at least a cylinder of 300 mm radius and 100 mm height. Pick-and-place trajectories are simulated by a 300 mm long straight line with velocities and acceleration varying along the path as shown in Fig. 5. The maximum acceleration is 100G and the maximum velocity is 11 m/s. Such a motion is simulated at different locations within the workspace (Fig. 6):

- from O_w to M_1 and from M_1 to O_w (trajectory 1),
- from M_2 to M_3 and from M_3 to M_2 (trajectory 2),
- from O_w to M_4 and from M_4 to O_w (trajectory 3),
- from M_5 to M_6 and from M_6 to M_5 (trajectory 4),

Three parameters are selected for the case study: r_b, l_i and L_i. A constant value of 0.05 m is chosen for r_{tp}; indeed, minimizing moving masses is of tremendous importance and the traveling plate has to be as small as possible: this value is considered to be the minimum size to install four pairs of S joints on the traveling plate. The other parameters can take the following values:

r_b = {0.120; 0.160; 0.200} m,
l_i = {0.200; 0.225; 0.250} m,
L_i = {0.500; 0.550; 0.600} m.

Moreover, the mass and the inertia of arms and forearms are functions of their length:

$$m_{i_f} = (0.500 \cdot L_i - 0.150)\ \text{kg}, \tag{50}$$

$$I_{i_{arm}} = (0.060 \cdot l_i - 0.007)\ \text{kg} \cdot \text{m}^2. \tag{51}$$

Two other dynamic parameters must be fixed: the mass of the traveling plate and the actuator inertia. For the simulation, the mass of the traveling plate is fixed to 0.2 kg. A mass of 0.25 kg is added to simulate a load. Actuator inertia is fixed to 0.004 kg·m^2 which corresponds to the inertia of high performance actuators which develop a peak torque of 127 N·m (RTMB0140-100 supplied by ETEL Motion Technology - http://www.etel.ch/).

B. Results

For each combination of the geometric parameters, the maximum torque required to realize the trajectories defined previously is computed. The altitude at which this maximum is minimum is also determined. Table VI presents the results ("-" means that the trajectories are not fully included in the reachable workspace).

First of all, several combinations of the geometric parameters give the same results of about 125 N·m. In particular, a 50 mm increase of L_i with a 25 mm decrease of l_i is seen to have not much effect on the maximum torque. A 50 mm increase of L_i with a 40 mm increase of r_b has not much effect either. Moreover, the increase of one parameter leads to an increase of the maximum torque. Considering this and the fact that the smallest possible robot is desired, the first line of Table VI seems to provide the best tradeoff between compactness and efficiency while guaranteing a reachable 300 mm $\times$ 100 mm cylindrical workspace as defined above.

TABLE VI

MAXIMUM TORQUE AS A FUNCTION OF THE GEOMETRIC PARAMETERS

r_b (m)	l_i (m)	L_i (m)	Γ_{max} (N·m)
0.120	**0.200**	**0.500**	**124**
0.120	0.200	0.550	133
0.120	0.200	0.600	142
0.120	0.225	0.500	134
0.120	0.225	0.550	143
0.120	0.225	0.600	152
0.120	0.250	0.500	143
0.120	0.250	0.550	152
0.120	0.250	0.600	162
0.160	0.200	0.500	-
0.160	0.200	0.550	-
0.160	0.200	0.600	129
0.160	**0.225**	**0.500**	**124**
0.160	0.225	0.550	132
0.160	0.225	0.600	140
0.160	0.250	0.500	133
0.160	0.250	0.550	141
0.160	0.250	0.600	149
0.200	0.200	0.500	-
0.200	0.200	0.550	-
0.200	0.200	0.600	-
0.200	0.225	0.500	-
0.200	0.225	0.550	-
0.200	0.225	0.600	131
0.200	0.250	0.500	-
0.200	0.250	0.550	133
0.200	0.250	0.600	141

C. Optimal R4 performance

The altitude at which the maximum torque is minimum is -0.53 m for the optimal R4. Hence, the workspace is included between z = -0.53 m and z = -0.43 m. Fig. 7 shows the min-max traveling plate acceleration for three planes: $z = \{$ -0.53 ; -0.48 ; -0.43 $\}$. It shows the influence of the position on this index since the minimum value is about 914 m/s^2 and the maximum value is about 1166 m/s^2: the lowest value is only 20% smaller than the maximum one. Fig. 8 shows the maximum possible traveling plate acceleration, equally for three planes: $z = \{$ -0.53 ; -0.48 ; -0.43 $\}$. Here also, the position influences the acceleration capability which is between 1470 m/s^2 and 1692 m/s^2 (13% change).

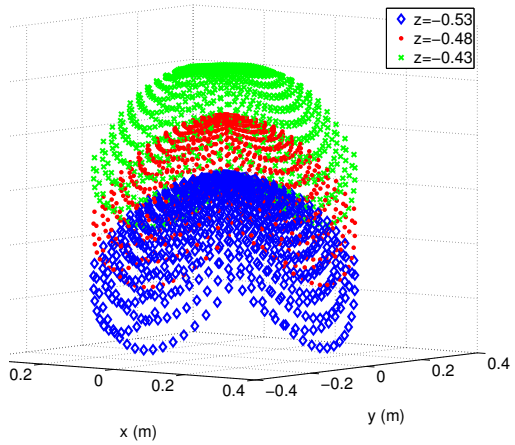

Fig. 7. Min-Max traveling plate acceleration of optimal R4 in planes $z = \{-0.53, -0.48, -0.43\}$

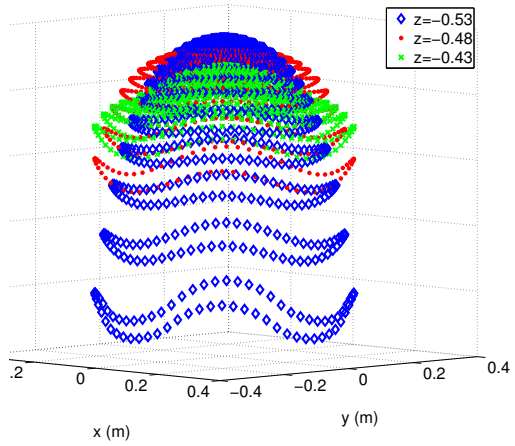

Fig. 8. Maximum possible traveling plate acceleration of optimal R4 in planes $z = \{-0.53, -0.48, -0.43\}$

Fig. 9 shows the torques needed to realize the four trajectories defined in section V-A.

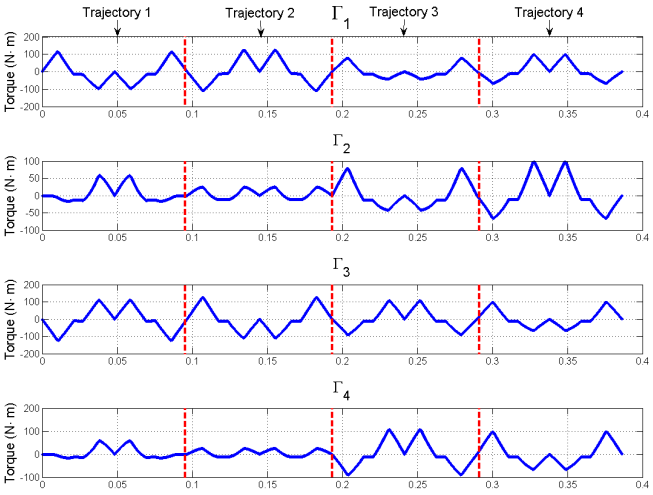

Fig. 9. Actuator torques needed for the defined four trajectories

VI. CONCLUSION

The work reported in this paper shows that actuation redundancy may be a realistic way to reach acceleration capabilities beyond that of PKM dedicated to pick-and-place applications. This study analyzing the case of a 3-dof/4-motors robot has been carried out with data corresponding to (i) classical trajectories similar to the one used in industrial equipments and (ii) mass and inertia parameters consistent with reasonable practical designs (see Fig. 10). It is worth noting that motor's data (torque, inertia) correspond to Direct Drives which will surely help in designing control laws since no backlash and very limited friction are expected.

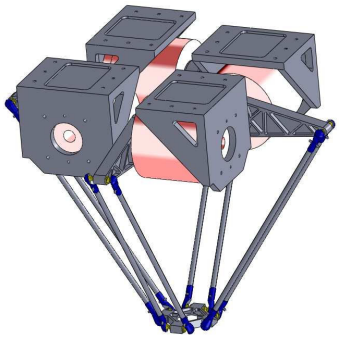

Fig. 10. CAD model of the optimal R4

VII. ACKNOWLEDGMENTS

This work has been partially funded by ANR Project "Objectif 100G".

REFERENCES

[1] R. Clavel, "Delta, a fast robot with parallel geometry," in *Proc. of the 18th International Symposium on Industrial Robots*, Lausanne, Switzerland, 1988, pp. 91–100.

[2] F. Pierrot, V. Nabat, O. Company, S. Krut, and P. Poignet, "Optimal design of a 4-dof parallel manipulator: From academia to industry," *IEEE Transactions on Robotics*, vol. 25 (2), pp. 213–224, 2009.

[3] F. Pierrot, C. Baradat, V. Nabat, O. Company, S. Krut, and M. Gouttefarde, "Above 40g acceleration for pick-and-place with a new 2-dof pkm," in *Proc. of the IEEE International Conference on Robotics and Automation (ICRA'09)*, Kobe, Japan, 2009, pp. 1794–1800.

[4] D. Corbel, "Contribution à l'amélioration de la précision des robots parallèles," Ph.D. dissertation, Université Montpellier II, Montpellier, France, 2008.

[5] T. Kokkinis and P. Millies, "A dynamically redundant parallel manipulator," in *Proc. of the International Symposium on Robotics and Manufacturing: Research, Education, and Applications (ISRAM'90)*, Burnaby, 1990, pp. 527–532.

[6] ——, "Kinetostatic performance of a dynamically redundant parallel robot," *International Journal of Robotics and Automation*, vol. 7, pp. 30–37, 1992.

[7] S. Kock and W. Schumacher, "A parallel x-y manipulator with actuation redundancy for high-speed and active-stiffness applications," in *Proc. of the IEEE International Conference on Robotics and Automation (ICRA'98)*, vol. 3, Leuven, Belgium, 1998, pp. 2295–2300.

[8] S. Kim, "Optimal redundant actuation of closed-chain mechanisms for high operational stiffness," in *Proc. of the IEEE International Conference on Intelligent Robots and Systems (IROS'00)*, vol. 1, Takamatsu, Japan, 2000, pp. 683–688.

[9] J. Wu, J. Wang, L. Wang, and T. Li, "Dynamic and control of a planar 3-dof parallel manipulator with actuation redundancy," *Mechanims and Machine Theory*, vol. 44 (4), pp. 835–849, 2009.

[10] F. Marquet, S. Krut, O. Company, and F. Pierrot, "Archi, a redundant mechanism for machining with unlimited rotation capacities," in *Proc. of the IEEE International Conference on Advanced Robotics (ICAR'01)*, Budapest, Hungary, August 22-25 2001, pp. 683–689.

[11] A. Muller, "Internal preload control of redundantly actuated parallel manipulators- its application to backlash avoiding control," *IEEE Transactions on Robotics*, vol. 21 (4), pp. 668–677, 2005.

[12] K. Nagai, M. Matsumoto, K. Kimura, and B. Masuhara, "Development of parallel manipulator "NINJA" with ultra-high-acceleration," in *Proc. of the IEEE International Conference on Robotics and Automation (ICRA'03)*, Taipei, Taiwan, September 2003, pp. 3678–1685.

[13] F. Marquet, "Contribution à l'étude de l'apport de la redondance en robotique parallèle," Ph.D. dissertation, Université Montpellier II, Montpellier, France, 2002.

[14] R. Clavel, "Conception d'un robot parallèle rapide à 4 degrés de liberté," Ph.D. dissertation, EPFL, Lausanne, Switzerland, 1991.

[15] A. Codourey, "Contribution à la commande des robots rapides et précis : application au robot delta à entrainement direct," Ph.D. dissertation, École polytechnique fédérale de Lausanne, 1991.

[16] V. Nabat, "Robots parallèles à nacelle articulée - du concept à la solution industrielle pour le pick-and-place," Ph.D. dissertation, Université Montpellier II, Montpellier, France, 2007.

[17] P. Chiacchio, "A new dynamic manipulability ellipsoid for redundant manipulators," *Robotica*, vol. 18, pp. 381–387, 2000.

[18] V. Garg, S. B. Nokleby, and J. A. Carretero, "Wrench capability analysis of redundantly actuated spatial parallel manipulators," *Mechanism and Machine Theory*, vol. 44, pp. 1070–1081, 2009.

[19] S. Bouchard, C. M. Gosselin, and B. Moore, "On the ability of a cable-driven robot to generate a prescribed set of wrenches," in *Proc. of the ASME Int. Design Engineering Technical Conf. and Computers and Information in Engineering Conf.*, no. Paper DETC2008-49518 [CD-ROM], Brooklyn, NY, 2008.

[20] Y. Zhao and F. Gao, "Dynamic performance comparison of the 8pss redundant parallel manipulator and its non-redundant counterpart - the 6pss parallel manipulator," *Mechanims and Machine Theory*, vol. 44 (5), pp. 991–1008, 2009.

[21] A. Muller, "Effects of geometric imperfections to the control of redundantly actuated parallel manipulators," in *Proc. of the IEEE International Conference on Robotics and Automation (ICRA'09)*, Kobe, Japan, 2009, pp. 1782–1787.